# CORRELATING ENVIRONMENTAL VARIABLES WITH RADON ACTIVITY IN AN IOWA CAVE

Lawrence E. Welch*, Anna Takashima, Monica B. Miguel, Brigitte C. Layug, Mark D. Jones, Christopher L. Beck
Knox College
Galesburg, Illinois, USA
lwelch@knox.edu

**Abstract**

Kemling Cave is located in Dubuque County, Iowa. It is a single-entrance cave with 3.51 km of surveyed passage. The entrance is gated, but done so in a manner that does not impede air exchange between the cave and the surface environment. Past work has shown that measurement of radon activity as a function of time in this cave displayed an extreme degree of variability. In this work, follow-up studies were designed and carried out to measure radon activity in parallel with a number of other environmental parameters, seeking to find which of the parameters had the strongest correlation with the radon activity.

*(1) The authors have received partial funding from Knox College to support the research leading to this publication, including allocations from the Billy Geer Fund, the Andrew W. Mellon Foundation, and the Paul K. and Evalyn Elizabeth Cook Richter Trusts.*

## Introduction

Seeking to better understand underground movement of radon and to improve measurement techniques for radon in caves has led to a research program at Knox College, largely working in the caves of northeast Iowa. The group has explored the use of continuous radon monitors (CRM, Welch, 2015) and electret ionization chambers (EIC, Welch, 2016) as sensors for in-cave measurements, and have utilized EIC units to produce a depth profile of radon activity (Welch, 2017).

Cave radon has proven to be a complex subject, largely due to the vast differences in structures and locations of caves. Jovanovič (1996) posited that caves that lay deep underground were expected to have minimal variations in radon activity over time, and caves that were closer to the surface would be expected to have variations in activity related to surface environmental parameters. The most commonly-described relationship of this type noted in the literature is a low-frequency (seasonal) variation in radon with surface temperature. This is typically expressed as low cave radon levels in the winter, and high cave radon in the summer. Since cave temperatures are largely constant with the seasons (Palmer, 2007), the standard trend is thought to be a function of the comparison of surface temperature to cave temperature. When the cave air is warmer and thus less dense than the surface air, the cave will vent itself via the chimney effect, releasing radon into the external atmosphere. When the cave is colder than the surface, the denser cave air is not ventilated efficiently, and radon tends to accumulate and remain in the cave until its decay. Examples of this behavior have been reported by Pinza-Molina (1999) in the Canary Islands, Jovanovič (1996) in Slovenia, Kowalczk (2010) in Florida, Langridge (2010) in the United Kingdom, Rovenska (2010) in the Czech Republic, and Lively (1995) in Minnesota. Hakl (1997), working in Hungary, stated that caves with small entrances to the surface were only impacted by surface temperature to a small degree. Counterexamples where radon was found to be lower in summer include Altamira Cave in Spain (Lario, 2005) and Mammoth Cave in Kentucky (Eheman, 1991). Altamira contains valuable cave paintings, the protection of which has led to artificial barriers altering atmospheric exchange with the surface. Mammoth Cave is the largest and arguably most complex cave in the world, featuring at present 24 different entrances, greatly complicating analysis (Klausner, 2018).

Higher frequency variations with radon activity have also been related to surface temperature, often diurnal in nature. Kowalczk (2010) and Lively (1995) reported temperature-correlated diurnal variations during the autumn, with a daytime increase in temperature and radon, followed by both dipping at night. Summer and winter trials did not show this same behavior. Rovenska (2010) reported the same proportional cycling of radon with temperature during the summer, but not during the winter. Attempts to make short-term correlations with surface atmospheric pressure have also been made. Hakl (1996), found that atmospheric pressure was an important driver of radon for largely vertical caves, but not so for caves classified as horizontal. The same group (Hakl, 1997) reported that atmospheric pressure was the main control parameter of radon in dead-end cave passages. Rovenska (2010) concluded that radon correlation with surface pressure was low in both summer and winter. Lively (1995) found that low surface pressure in the winter produced spikes of radon activity to high levels from a low baseline value, but the magnitude of the radon change did not follow that of the pressure change and that the radon spikes always correlated with pressure drops, but pressure drops did not always produce radon spikes. Summer produced a high radon baseline value with occasional troughs to lower levels, but they did not correlate with surface pressure. Although not a cave-based study, but looking at

a similar phenomenon, Kotrappa (2013) showed that the extremely low surface pressure generated by Superstorm Sandy caused a strong negative correlation with radon measurement in a basement held in closed-house conditions, as the low pressure pulled radon out of the basement walls and surrounding soil more effectively. On the other hand, Kowalczyk (2010) found the opposite behavior for a small Florida cave during a tropical storm for a small cave open to the atmosphere. This observation was thought to be due to an increase in ventilation of the cave.

Most of the temperature and pressure correlations with radon have been explained as being due to the creation of air movement, and the resultant advection has been described as the most important factor controlling radon transport (Hakl, 1996). Advection of radon in caves has largely been inferred from measurements of other environmental variables, as opposed to measured directly. Kowalczyk (2010) measured wind velocities in some Florida caves, and noted higher wind velocities were seen in the winter, producing better cave ventilation and lower radon levels. The opposite behavior was seen in the summer.

Kemling Cave lies near Dubuque, IA in limestone of Ordovician Age, and it has 3.51 kilometers of surveyed passages (Klausner, 2018). It is on private property and a non-commercial entity. Unlike many of the studies set in commercial caves, there is no electrical power source in the cave and any sensors deployed here have to be battery-powered. The cave has a single entrance of cross-section circa 1 $m^2$ that is gated, but not sealed, to facilitate bat movement in and out of the cave. As such there is open communication with the external atmosphere. Immediately inside the entrance is a 7.19 m vertical pit, followed by essentially horizontal passage to the point where the sensors were placed in this study. The known cave passages are largely at a depth of 20 m or less below the surface, and the cave can best be described as a horizontal maze. The goal of this study was to measure radon in the entry passage of this cave while concurrently measuring environmental variables at the same site in the cave and on the surface outside the cave, looking for significant correlations within a time frame of circa one week.

## Materials and Methods

Temporal measurements of radon activity were undertaken using Radon Scout Plus continuous radon monitors and Radon Vision software version 6.0.7 (Rad Elec Inc.). Scout Plus measurements were acquired at 1 hour increments. The Scout Plus units were deployed in Tyvek® envelopes to protect them from mud and water while in the cave. Once in the Tyvek®, the Scout Plus units were packaged in their thermoplastic case for transport and deployment in the cave. Prior work demonstrated that both the envelopes and the thermoplastic cases are transparent to radon (Stieff, 2012 and Welch, 2015) and do not impact measured levels. Independent measurements of pressure, temperature, and relative humidity were made using OM-CP-PRTEMP101 [PRTEMP] and OM-CP-PRHTEMP101 [PRHTEMP] sensors with OM-CP Data Logging software (OMEGA Engineering). The measurements were acquired at 5 minute increments. When used on the surface, the PRTEMP and PRHTEMP units were clamped underneath a board suspended between two buckets, thus protecting them from direct sunlight exposure, yet maintaining free air circulation. When used in the cave the PRTEMP and PRHTEMP units were deployed in Tyvek® envelopes to protect them from mud and water. When PRTEMP units were used on the surface, corresponding humidity data was available from

compiled tabulations at the Weather Underground web site for the nearby Dubuque Regional Airport, approximately 7 km from the cave (Weather Underground, 2018).

Wind direction and velocity was measured with a Windsonic Option 2 from Gill Instruments Ltd. A SpaceLogger® .W10 WindLogger from Richard Paul Russell Limited was used to record the data onto an SD card. Various sizes and models of 12V lead-acid batteries were used to power the detector head and logging unit. The Windsonic sensor head was aligned properly with magnetic north using a Suunto KB-14 compass. Since the magnetic declination for the location and time frame being used was very close to +1 degree, which was easily within the uncertainty of positioning the Windsonic in the cave, it was a safe assumption that the Windsonic was also closely aligned with true north. The WindLogger and battery were protected during trials and the entire wind sensor apparatus was transported in the cave inside a modified Trolling Motor Power Center from Minn Kota, a thermoplastic case with external electrical connection jacks which had been designed to protect marine batteries from the elements. The Windsonic measurements were acquired at 1 second increments. Wind direction was given in degrees representing the direction the wind originated. The Windsonic could only determine wind direction if the wind velocity during the corresponding time segment was at least 0.05 m/s, otherwise the data bin for direction was left blank.


Figure (1): Sensor setup, Kemling Cave entry passage, facing east.

All of the sensors were mounted on tripods and placed near each other circa 1.0 m above the cave floor and 0.5 m from each side wall, which placed them generally in the center of the cave

passage. A location approximately 20 meters into the cave was chosen as the site for this study. Figure (1) shows the complete assembled sensor array in the Kemling Cave entry passage.

Wet air density values in units of $kg/m^3$ were calculated from measured data in the manner given by Omnicalculator (2018). Pearson's R values and Pearson's P values were calculated with Microsoft Excel. Correlations were deemed to be statistically significant at the 95% confidence level if the P value was found to be less than 0.05. For wind calculations, the cave was considered to be exhaling for Windsonic angles between 70 and 110 degrees, and inhaling for angles between 250 and 290 degrees.

## Results and Discussion

Initial trials looking at radon variation as a function of time were undertaken in Coldwater Cave, Winneshiek County, Iowa. The entrances to this cave all achieve an airtight seal, and the cave itself features only minimal air movement as a result. In addition, nearly all Coldwater passages are deep below the surface. The high-frequency variation in measured radon activity was minimal, consistent with the prediction by Jovanovič (1996). When the same experiment was run in the entry passage of Kemling Cave in August of 2012 as Experiment 18, a very different response was noted (Figure (2)) as befit a shallower cave that was open to the surface. The radon activity was seen to vary between 96 and 353 pCi/L, and the plot suggested something close to a regular pattern to the variation. Although fairly regular, the variation did not look to be diurnal in nature, given the time values.

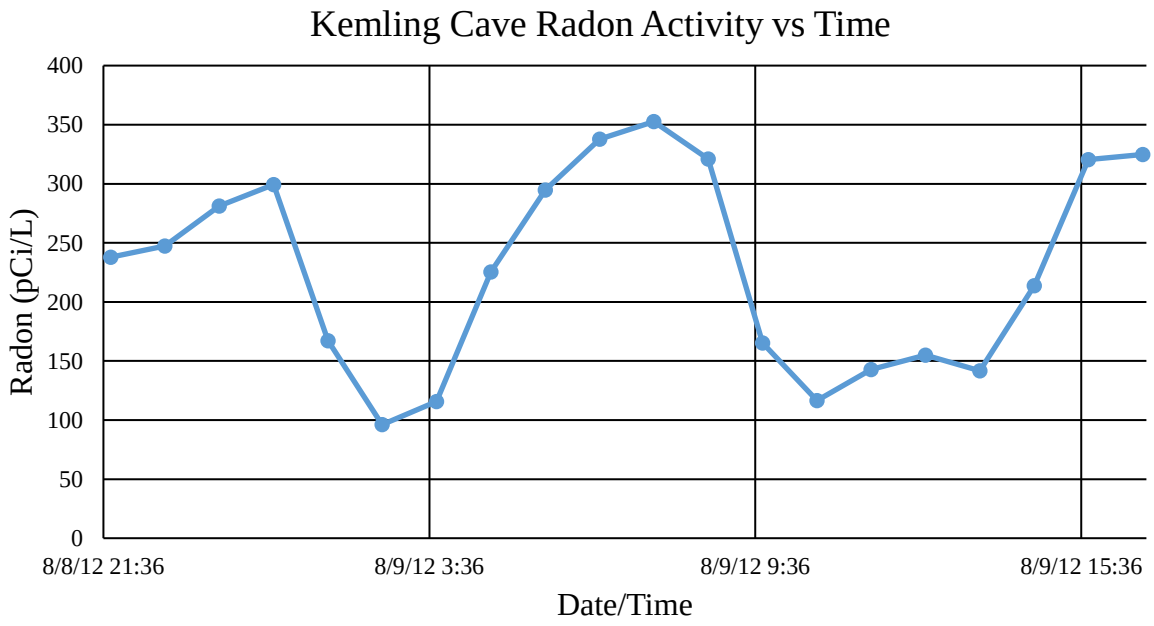


Figure (2): Kemling Cave radon activity vs. time, August 2012, Experiment 18.

The study was repeated with a much longer duration and with the inclusion of additional sensors. Radon was measured at the same position in the Kemling entry passage, but atmospheric

pressure, temperature, and humidity were measured concurrently at the same location in the cave and also on the surface just outside the cave.

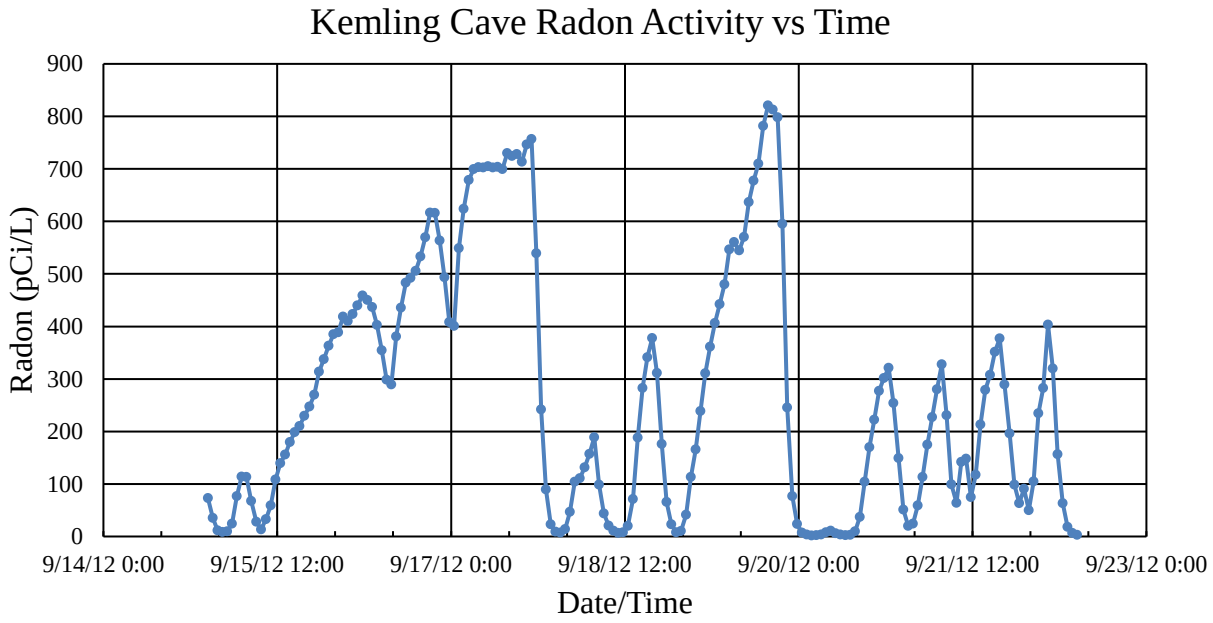


Figure (3): Kemling Cave radon activity vs. time, September 2012, Experiment 20.

The subsequent trial, Experiment 20 from September 2012, extended for 181 hours, and the radon activity was hypervariable during this time span (Figure (3)), yet less suggestive of patterned behavior than that seen in Figure (2). Having both pressure and temperature data for the surface and the in-cave sampling site allowed radon activity correlations to be found with each, as well as radon correlations with $\Delta P$ and $\Delta T$. Since relative humidity information was also available, the wet air density could be calculated and correlated as well. Correlation coefficients (Pearson's R value) and Pearson's P values for each category are given in Figure (4), sorted from largest to smallest absolute R value. All of the correlations were found to be statistically significant, yet no extremely high R values were found. The variable with the strongest radon activity correlation was cave temperature. However, it was hard to take this value too seriously, given that cave temperature was expected (Palmer, 2007) to be almost constant. An evaluation of the cave temperature data stream for this experiment showed that the set had a relative standard deviation of only 0.353%, so despite the high R value, it was unlikely to be a significant factor driving change in radon levels. The second-highest correlation was with surface pressure. That the correlation was negative was also expected: the partial vacuum of low pressure would be expected to pull the radon gas out of the rock strata more effectively, enriching the content in air much like that reported by Kotrappa (2013). What was surprising was that the correlation between surface pressure and radon was stronger than that with the pressure measured at the sampling site in the cave, as it would seem that the pressure in the immediate vicinity would be the driver that pulled radon out of the rock strata. An overlay of the cave pressure and the surface pressure on the radon variation (Figure (5)), illustrates that the cave pressure tended to mirror the surface pressure with a bit of a time lag and a muted change in

magnitude. Replicate trials affirmed that the correlation with cave pressure tended to be slightly poorer than with surface pressure, although the gap was typically smaller than in this trial.

| Parameter - 5 min avg | Exp 20 R Value | Exp 20 P Value | Significant? |
|---|---|---|---|
| cave temp | -0.525 | 3.27E-14 | Y |
| surf pressure | -0.503 | 5.09E-13 | Y |
| surf wet air density | -0.482 | 6.38E-12 | Y |
| Δwet air density (surf-cave) | -0.437 | 7.77E-10 | Y |
| Δpressure (surf - cave) | -0.432 | 1.29E-09 | Y |
| Δtemp (surf - cave) | 0.413 | 7.59E-09 | Y |
| surf temp | 0.400 | 2.47E-08 | Y |
| cave pressure | -0.342 | 2.53E-06 | Y |
| cave wet air density | -0.251 | 6.39E-04 | Y |

Figure (4): Environmental variable correlation with radon activity, Kemling Cave, September 2012, Experiment 20.

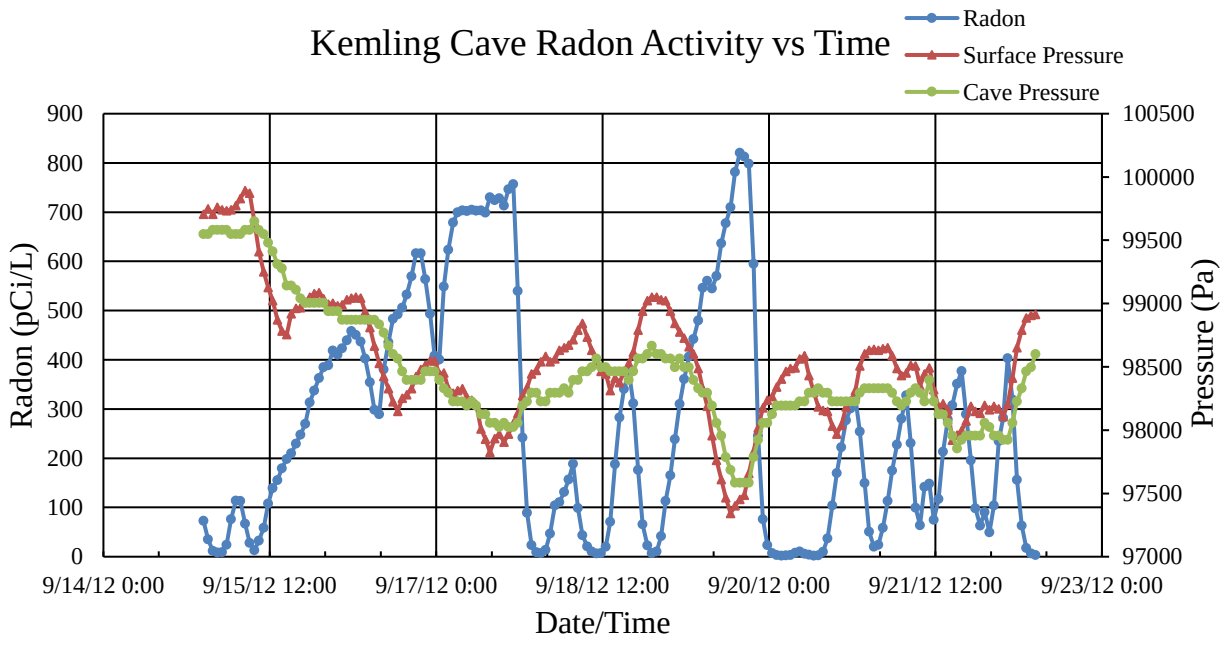


Figure (5): Radon activity overlaid by surface and cave pressure, Kemling Cave, September 2012, Experiment 20.

The correlation with surface temperature was smaller than that with surface pressure, and positive in sign. This was logical given that comparison of corresponding surface pressure and surface temperature values yielded a significant negative correlation, and consistent with reports for autumn behavior from Kowalczk (2010) and Lively (1995). Radon activity correlation with Δtemperature (surface-cave) was almost the same as that seen with just surface temperature,

which follows given that the cave temperature was nearly constant. Since pressure differentials are the most important factor driving cave wind (Palmer, 2007), it was thought that the Δpressure correlation would serve as a predictor of how cave wind impacted radon, which was expected to be high. If the cave was inhaling, it would tend to breathe in surface air that was very low in radon, dropping the radon activity in the entry passage. If it was exhaling, it would tend to propel air from deep in the cave through the entry passage, keeping the radon activity high in this region. However, the Δpressure correlation was smaller than that seen with surface pressure. Since the entrance to the cave was a vertical shaft, air density values were calculated and correlations sought with radon activity. The cave wet air density correlation, though statistically significant, was the smallest of any of the variables tested, whereas the surface wet air density had a fairly high R value. The correlation was also a negative one, so more dense surface air produced small radon activities, which might follow that dense air on the surface would tend to be pulled down the entry shaft, diluting the entry passage radon with low-radon outside air.

| | **surf pressure** | **cave pressure** | **Δpressure (surf - cave)** | **surf temp** | **cave temp** | **surf wet air density** |
|---|---|---|---|---|---|---|
| | | | | | | |
| **R overall** | -0.503 | -0.342 | -0.432 | 0.400 | -0.525 | -0.482 |
| **R daytime** | -0.635 | -0.505 | -0.305 | 0.264 | -0.513 | -0.398 |
| **R nighttime** | -0.291 | -0.147 | -0.599 | 0.664 | -0.531 | -0.671 |

Figure (6): Environmental variable day/night subset correlations with radon activity, Kemling Cave, September 2012, Experiment 20.

In all, the results of this trial did not identify a clear culprit that was driving radon variations. In an attempt to gather a more nuanced view, the data was broken into day and night subsets, and the correlations with radon activity calculated for each segment as shown in Figure (6). The correlations for cave temperature changed minimally no matter how the segments were cleaved, reinforcing the perception that this category was not yielding any useful information. It was notable that the magnitude of both pressure correlations went up significantly during daylight hours, and were much poorer at night. The correlations for surface temperature, density, and for ΔP (surf-cave) did the opposite – presenting much higher absolute R values at night. In general, every evening the sun would set, surface temperature would drop, while the surface pressure would rise correspondingly and the cave pressure would do the same after a time lag. This would presumably lead to an inhalation by the cave of low-radon outside air, and less suction pulling radon out of the rock strata, both factors tending to produce low radon activity in the entry passage. Each morning with sunrise, the surface temperature would go up and the surface pressure would drop, followed after a lag by a reduction in cave pressure. This would presumably lead to an exhalation by the cave, pulling high-radon air from deep in the cave out the entrance and producing more suction pulling radon out of the rock strata, both factors tending to produce high radon activity in the entry passage. However, the vagaries of changing temperature and pressure from a continual stream of weather patterns were then superimposed upon the top of the diurnal pattern, greatly complicating the actual output. It should be noted that the execution of the experiment during September was important here, as in the height of

summer the surface low temperatures would never reach cave temperature and in the middle of winter the surface high temperatures would never reach cave temperature.

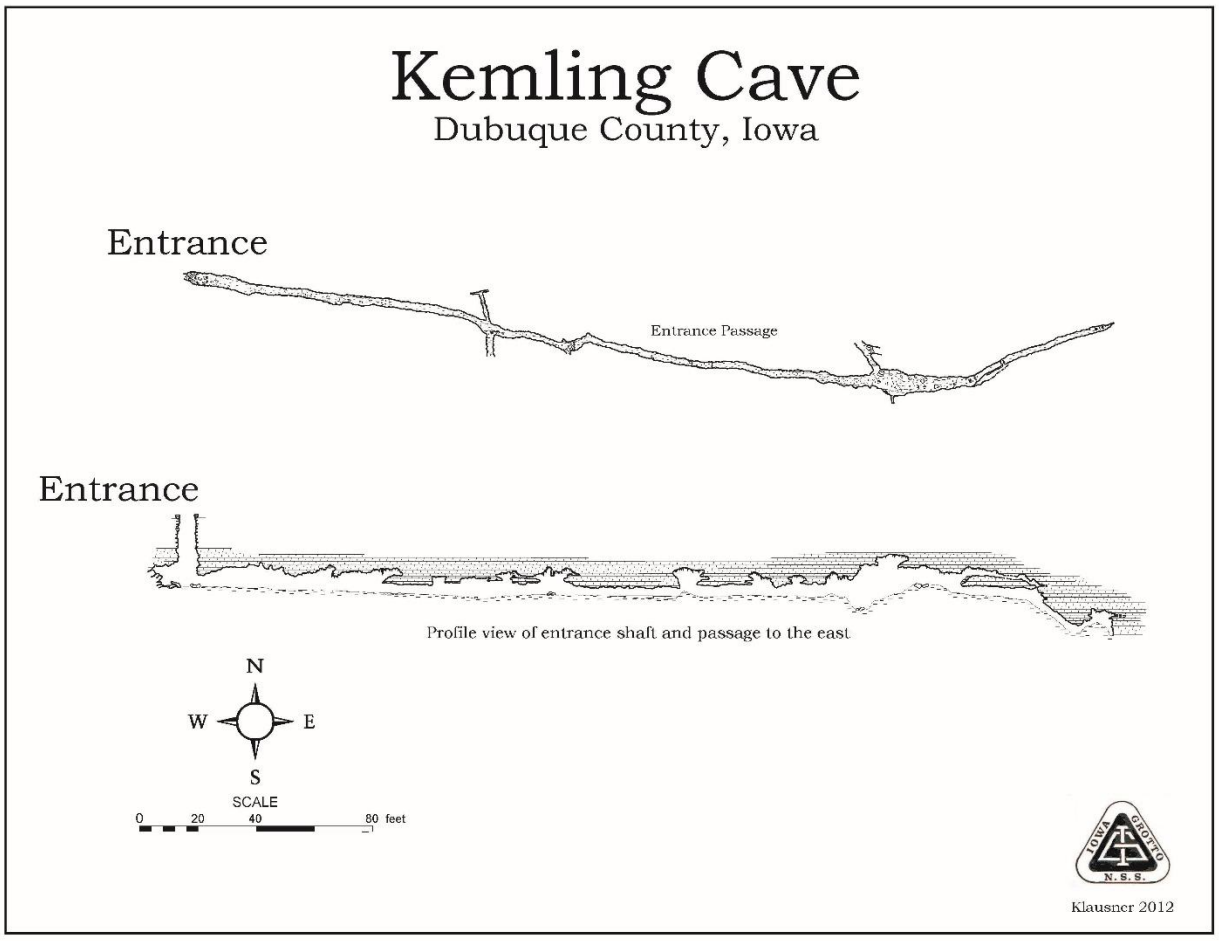


Figure (7): Map of the entrance passage, Kemling Cave, courtesy of Ed Klausner.

It was expected that air movement in the cave was an important factor driving radon variations, but one outcome of Experiment 20 was that there was not absolute confidence that the Δpressure measurement was serving as a good proxy for cave wind information. To better understand the role of wind, a Windsonic unit that measured wind velocity and wind direction was obtained and added to the in-cave sensor array, and the prior experiment repeated as Experiment 35 in July 2013, a 143-hour trial. A map of the entrance passage of Kemling cave (see Figure (7)) shows that the passage is narrow and closely aligned with an east-west axis. Thus the wind direction measurements would be expected to be clustered around 90 degrees (cave exhaling) and 270 degrees (cave inhaling). As such, it was expected that the wind direction would provide a negative correlation with radon activity. Since wind velocity and wind direction were separate measurements, a composite category, the net wind vector, was calculated that would blend both parameters. This value was found by taking the sine of the wind direction multiplied by the wind velocity for the same time increment. This would give the net wind vector a positive value for the cave exhaling wind and a negative value for the cave inhaling wind. It was expected that this

new parameter would give the strongest correlation with radon activity, with a positive sign. Since the wind data were collected once per second, this information was averaged over a minimum 5-minute span such that these values matched the frequency of the pressure, temperature, and humidity data.

| **Parameter - 5 min avg** | **Exp 20 R Value** | **Exp 35 R Value** | **Exp 35 P Value** | **Significant?** |
|---|---|---|---|---|
| surf pressure | -0.503 | -0.620 | 1.84E-16 | Y |
| surf wet air density | -0.482 | -0.120 | 1.54E-01 | N |
| Δpressure (surf - cave) | -0.432 | 0.051 | 5.48E-01 | N |
| surf temp | 0.400 | 0.044 | 6.07E-01 | N |
| cave pressure | -0.342 | -0.591 | 9.73E-15 | Y |
| cave wind direction | | -0.125 | 3.20E-01 | N |
| cave wind velocity | | 0.376 | 4.03E-06 | Y |
| cave net wind vector | | 0.175 | 1.64E-01 | N |

Figure (8): Environmental variable correlation with radon activity, Kemling Cave, Experiment 35 vs. Experiment 20.

Notwithstanding the change in season, hypervariable radon activity was still observed for Experiment 35. Figure (8) shows the outcome of Experiment 35 compared to the prior data from Experiment 20. Categories that used the nearly-constant cave temperature value (cave T, ΔT, Δdensity) were removed from consideration in this experiment. Surface pressure still showed the strongest correlation with radon activity, it was still a negative correlation, and was only trailed slightly in absolute terms by the correlation with cave pressure. Correlations with surface density, surface temperature and ΔP (surf-cave) dropped to the point that they were not statistically significant. The great expectation of strong correlation with wind was only partially fulfilled, with wind direction and net wind vector showing insignificant correlations. Only wind velocity had a significant correlation, positive in sign, yet this parameter was independent of wind direction, which was observed to change during the trial. After viewing overlay plots of the environmental variables vs. radon activity, it was postulated that the wind parameters were in fact impacting radon levels, but the R values were not properly reflecting that because the impact on radon was delayed in time. To evaluate this, the radon activity data was offset to earlier time values one hourly step at a time, and the correlations recalculated. Figure (9) shows the time-offset correlations for Experiment 35. The pressure correlations did not improve nor change greatly with the offset, but all of the wind categories improved strikingly to maxima at 3-hour offsets. The correlation with wind velocity was now the largest of any of the environmental variables. The correlation with wind direction, although less than the pressure correlations, was now significant and still negative. The negative value matched expectations, as wind at 90 degrees would mean air from the cave flooding the entrance passage and leading to high radon levels, whereas 270 degree wind would mean surface air was being pulled into the entrance passage, leading to low radon levels. The net wind vector R value was also much larger, significant, and positive in nature due to the sine of 90 degrees being a large positive and the sine of 270 degrees being a large negative.

| Parameter - 5 min avg | Exp 35 R value real time | Exp 35 R value 1 hour offset | Exp 35 R value 2 hour offset | Exp 35 R value 3 hour offset | Exp 35 R value 4 hour offset |
|---|---|---|---|---|---|
| surf pressure | -0.620 | -0.623 | -0.594 | -0.531 | -0.452 |
| surf wet air density | -0.120 | -0.166 | -0.192 | -0.185 | -0.157 |
| Δpressure (surf - cave) | 0.051 | 0.010 | -0.001 | 0.035 | 0.086 |
| surf temp | 0.044 | 0.086 | 0.111 | 0.105 | 0.080 |
| cave pressure | -0.591 | -0.580 | -0.549 | -0.500 | -0.442 |
| cave wind direction | -0.125 | -0.279 | -0.388 | -0.404 | -0.353 |
| cave wind velocity | 0.376 | 0.510 | 0.630 | 0.664 | 0.624 |
| cave net wind vector | 0.175 | 0.344 | 0.462 | 0.485 | 0.430 |

Figure (9): Environmental variable correlation with radon activity, Kemling Cave, Experiment 35, July 2013, evaluating correlations with radon data offset to earlier times.

| Parameter/Offset Time | 5 min avg | 60 min avg | 120 min avg | 180 min avg | 240 min avg | 300 min avg | 360 min avg | 420 min avg |
|---|---|---|---|---|---|---|---|---|
| **Surface Pressure** | | | | | | | | |
| Real Time | -0.620 | -0.627 | -0.624 | -0.609 | -0.585 | -0.557 | -0.525 | -0.493 |
| vs Radon 1 hr offset | -0.623 | -0.616 | -0.594 | -0.565 | -0.532 | -0.498 | -0.463 | -0.430 |
| vs Radon 2 hr offset | -0.594 | -0.569 | -0.534 | -0.498 | -0.461 | -0.425 | -0.392 | -0.364 |
| vs Radon 3 hr offset | -0.531 | -0.497 | -0.456 | -0.419 | -0.383 | -0.351 | -0.323 | -0.301 |
| **Cave Pressure** | | | | | | | | |
| Real Time | -0.591 | -0.591 | -0.581 | -0.563 | -0.540 | -0.516 | -0.493 | -0.473 |
| vs Radon 1 hr offset | -0.580 | -0.569 | -0.547 | -0.520 | -0.494 | -0.470 | -0.449 | -0.410 |
| vs Radon 2 hr offset | -0.549 | -0.527 | -0.497 | -0.466 | -0.442 | -0.420 | -0.401 | -0.365 |
| vs Radon 3 hr offset | -0.500 | -0.472 | -0.440 | -0.409 | -0.389 | -0.371 | -0.354 | -0.323 |
| **Cave Wind Direction** | | | | | | | | |
| Real Time | -0.125 | -0.163 | -0.267 | -0.316 | -0.327 | -0.325 | -0.302 | -0.262 |
| vs Radon 1 hr offset | -0.279 | -0.318 | -0.375 | -0.382 | -0.367 | -0.342 | -0.310 | -0.267 |
| vs Radon 2 hr offset | -0.388 | -0.394 | -0.412 | -0.404 | -0.377 | -0.343 | -0.309 | -0.263 |
| vs Radon 3 hr offset | -0.404 | -0.400 | -0.405 | -0.395 | -0.364 | -0.333 | -0.299 | -0.250 |

**Cave Wind Velocity**

| | | | | | | | | |
|---|---|---|---|---|---|---|---|---|
| Real Time | 0.376 | 0.443 | 0.560 | 0.663 | 0.737 | 0.784 | 0.811 | 0.820 |
| vs Radon 1 hr offset | 0.510 | 0.607 | 0.706 | 0.772 | 0.807 | 0.819 | 0.816 | 0.801 |
| vs Radon 2 hr offset | 0.630 | 0.716 | 0.774 | 0.798 | 0.799 | 0.782 | 0.757 | 0.733 |
| vs Radon 3 hr offset | 0.664 | 0.735 | 0.752 | 0.744 | 0.719 | 0.685 | 0.656 | 0.636 |

**Cave Net Wind Vector**

| | | | | | | | | |
|---|---|---|---|---|---|---|---|---|
| Real Time | 0.175 | 0.213 | 0.324 | 0.388 | 0.415 | 0.433 | 0.417 | 0.390 |
| vs Radon 1 hr offset | 0.344 | 0.380 | 0.449 | 0.470 | 0.468 | 0.452 | 0.422 | 0.391 |
| vs Radon 2 hr offset | 0.462 | 0.471 | 0.498 | 0.499 | 0.475 | 0.444 | 0.411 | 0.381 |
| vs Radon 3 hr offset | 0.485 | 0.488 | 0.492 | 0.483 | 0.449 | 0.420 | 0.390 | 0.359 |

Figure (10): Environmental variable correlation with radon activity, Kemling Cave, Experiment 35, July 2013, evaluating changes in environmental variable integration time and radon offset to earlier times.

After observing the impact of the offset time, an evaluation was made regarding the time frame over which the environmental parameter value was averaged. Given the significant lag times observed for the wind values, would the correlations improve if the average were calculated over a longer time frame rather than the standard 5-minute window? Figure (10) shows correlations from Experiment 35 over a range of time values. The pressure variables do not change R value sign, and do not change much in magnitude before slowly fading to smaller values. The wind categories all show greatly enhanced correlations with longer integration times, with the velocity correlation continually increasing with integration time and the direction and net wind vector values maxing out at a 3-4 hour integration window. Some of the longer time frame correlations with wind velocity exceeded 0.8.

Although the addition of the time offsets and the varied integration time frames for the environmental variable added greatly to the understanding of the experimental results, the wind categories still yielded puzzling output. The net wind vector data were expected to produce the strongest correlations, yet instead they ended up being smaller than the wind velocity correlations, which did not factor in the wind direction whatsoever. A deep look into the dataset illuminated a potential malefactor. As noted in the Materials and Methods section, the wind sensor in use could only determine wind direction if the wind velocity was at a minimum 0.05 m/s. If velocity was below this value, an empty bin would be recorded for the wind direction, which also factored into the calculated net wind vector. The environmental conditions during Experiment 35 were such that a large number of the data bins were bereft of wind direction values – nearly 75% of the overall total. Figure (11A) illustrates this situation. Giant blank swaths in the data set for wind direction and net wind vector meant that large time intervals during the trial had no useful data, doubtlessly weakening the utility of any calculations based on these parameters. It also meant that the correlation coefficient was being calculated with a much smaller N value than the other environmental parameters that filled all of the data bins. Finally, there was some question about whether the longer integration times yielded higher correlations for the wind categories because they indeed were a cumulative factor impacting radon levels, or

whether it just better masked the inherent weakness of the wind data set by increasing the likelihood that the wind direction bin would contain data by averaging over a wider time frame.

**A**

| **Experiment 35** | **Day 1 (partial)** | **Day 2** | **Day 3** | **Day 4** | **Day 5** | **Day 6** | **Day 7 (partial)** |
|---|---|---|---|---|---|---|---|
| | **07/25/13** | **07/26/13** | **07/27/13** | **07/28/13** | **07/29/13** | **07/30/13** | **07/31/13** |
| **Wind direction % filled bins** | 36.77 | 41.04 | 30.76 | 13.86 | 2.84 | 28.69 | 34.66 |
| **Cumulative % filled bins** | 36.77 | 40.07 | 36.01 | 29.29 | 23.13 | 24.18 | 25.85 |

**B**

| **Experiment 44** | **Day 1 (partial)** | **Day 2** | **Day 3** | **Day 4** | **Day 5** | **Day 6** | **Day 7** |
|---|---|---|---|---|---|---|---|
| | **11/06/13** | **11/07/13** | **11/08/13** | **11/09/13** | **11/10/13** | **11/11/13** | **11/12/13** |
| **Wind direction % filled bins** | 89.03 | 44.83 | 69.36 | 79.51 | 85.64 | 92.52 | 88.64 |
| **Cumulative % filled bins** | 89.03 | 59.25 | 63.32 | 67.97 | 71.91 | 75.67 | 77.67 |
| | | | | | | | |
| | **Day 8** | **Day 9 (partial)** | | | | | |
| | **11/13/13** | **11/14/13** | | | | | |
| **Wind direction % filled bins** | 95.51 | 79.22 | | | | | |
| **Cumulative % filled bins** | 80.05 | 79.99 | | | | | |

Figure (11): Comparing the percentage of empty data bins for the wind direction category, Kemling Cave, Experiments 35 and 44.

| Parameter - 5 min avg | Exp 20 R Value | Exp 35 R Value | Exp 44 R Value | Exp 44 P Value | Significant? |
|---|---|---|---|---|---|
| surf pressure | -0.503 | -0.620 | -0.476 | 7.59E-15 | Y |
| surf wet air density | -0.482 | -0.120 | -0.272 | 2.06E-05 | Y |
| Δpressure (surf - cave) | -0.432 | 0.051 | -0.281 | 1.11E-05 | Y |
| surf temp | 0.400 | 0.044 | 0.168 | 9.36E-03 | Y |
| cave pressure | -0.342 | -0.591 | -0.446 | 4.68E-13 | Y |
| cave wind direction | | -0.125 | -0.548 | 7.21E-16 | Y |
| cave wind velocity | | 0.376 | 0.240 | 7.83E-04 | Y |
| cave net wind vector | | 0.175 | 0.623 | 3.09E-21 | Y |

Figure (12): Environmental variable correlation with radon activity, Kemling Cave, Experiment 44 vs. prior experiments.

To probe the impact of the empty bins on the wind correlations, an evaluation was made of one of the replicate trials of this experiment, Experiment 44 from November of 2013. As can be seen in Figure (11B), nearly 80% of the data bins for wind direction and net wind vector were filled in this trial, a much higher value than seen in the prior experiment. Figures (12) and (13) give the output from this experiment, and the enhancement in wind direction and net wind vector correlations were evident. The net wind vector had the strongest correlation for the 5-minute average, and, as before, longer integration periods and adding offset periods improved the quality of the correlation, although only modestly. The wind direction behaved in a similar manner, and only trailed the net wind vector in correlation strength by a small amount. The pressure values had somewhat smaller R values than in the previous trial, but they had the same sign, were still significant, and once again looked to be the most important of the non-wind environmental variables. Like in the other trials, the surface pressure had a stronger correlation than the cave pressure, and the addition of longer integration times and the addition of offset periods did not improve the pressure correlations. Correlations with surface density, surface temperature and ΔP (surf-cave) were statistically significant, in contrast to the prior trial, but all were small and did not look to be important. Following on the heels of the extremely high wind velocity correlation from Experiment 35, the same correlation in Experiment 44 produced much more modest R values. They were still positive and still significant, but now were smaller than the R values for either of the pressure values and nowhere close to the R values for the other wind parameters. A deep look into the dataset helped to explain this outcome. During Experiment 35, the ratio of data points where the cave was inhaling divided by points where it was exhaling was 131.5. The same ratio calculated for the duration for Experiment 44 gave a value of only 1.329. So for Experiment 35, the extremely high correlation of wind velocity, despite its lack of directional information, could be explained by the fact that the cave was inhaling through most of the experiment (or at least during the time sectors where the wind velocity was high enough to allow wind direction to be registered). There was a much more even balance of inhaling and exhaling during Experiment 44, and the velocity did not correlate as well without the directional information, whereas the net wind vector, factoring in both direction and velocity, had the strongest correlation. This latter case with a more balanced proportion of inhaling and exhaling is likely to better represent normal behavior of the cave environment. Finally, the wind variables all saw enhancement as the integration period was extended during Experiment 44, but not as

dramatically as that seen in Experiment 35. It seems likely that part of the dramatic enhancement in Experiment 35 was due to the longer integration time frame increasing the likelihood that a bin would have data, given the vast number of empty bins for each individual reading. Figure (14) illustrates the high degree of net wind vector correlation with radon for this experiment.

| **Parameter/Offset Time** | **5 min avg** | **60 min avg** | **120 min avg** | **180 min avg** | **240 min avg** | **300 min avg** | **360 min avg** | **420 min avg** |
|---|---|---|---|---|---|---|---|---|
| **Surface Pressure** | | | | | | | | |
| Real Time | -0.476 | -0.460 | -0.445 | -0.428 | -0.408 | -0.388 | -0.366 | -0.343 |
| vs Radon 1 hr offset | -0.445 | -0.426 | -0.407 | -0.386 | -0.365 | -0.342 | -0.319 | -0.294 |
| vs Radon 2 hr offset | -0.406 | -0.384 | -0.363 | -0.340 | -0.317 | -0.292 | -0.267 | -0.242 |
| vs Radon 3 hr offset | -0.361 | -0.337 | -0.314 | -0.290 | -0.265 | -0.240 | -0.214 | -0.188 |
| **Cave Pressure** | | | | | | | | |
| Real Time | -0.446 | -0.431 | -0.416 | -0.400 | -0.381 | -0.362 | -0.341 | -0.319 |
| vs Radon 1 hr offset | -0.416 | -0.397 | -0.379 | -0.360 | -0.339 | -0.317 | -0.295 | -0.271 |
| vs Radon 2 hr offset | -0.378 | -0.356 | -0.336 | -0.315 | -0.293 | -0.269 | -0.245 | -0.221 |
| vs Radon 3 hr offset | -0.335 | -0.311 | -0.289 | -0.266 | -0.243 | -0.218 | -0.194 | -0.169 |
| **Cave Wind Direction** | | | | | | | | |
| Real Time | -0.548 | -0.567 | -0.587 | -0.604 | -0.617 | -0.628 | -0.635 | -0.642 |
| vs Radon 1 hr offset | -0.587 | -0.597 | -0.611 | -0.622 | -0.629 | -0.634 | -0.640 | -0.645 |
| vs Radon 2 hr offset | -0.607 | -0.608 | -0.622 | -0.627 | -0.630 | -0.633 | -0.638 | -0.644 |
| vs Radon 3 hr offset | -0.611 | -0.614 | -0.623 | -0.624 | -0.626 | -0.629 | -0.635 | -0.641 |
| **Cave Wind Velocity** | | | | | | | | |
| Real Time | 0.240 | 0.252 | 0.280 | 0.307 | 0.337 | 0.365 | 0.388 | 0.405 |
| vs Radon 1 hr offset | 0.283 | 0.290 | 0.316 | 0.345 | 0.373 | 0.394 | 0.409 | 0.420 |
| vs Radon 2 hr offset | 0.309 | 0.322 | 0.353 | 0.379 | 0.397 | 0.410 | 0.418 | 0.424 |
| vs Radon 3 hr offset | 0.346 | 0.360 | 0.384 | 0.399 | 0.407 | 0.413 | 0.417 | 0.419 |
| **Cave Net Wind Vector** | | | | | | | | |
| Real Time | 0.623 | 0.650 | 0.675 | 0.696 | 0.715 | 0.730 | 0.741 | 0.748 |
| vs Radon 1 hr offset | 0.666 | 0.689 | 0.707 | 0.724 | 0.737 | 0.746 | 0.751 | 0.754 |
| vs Radon 2 hr offset | 0.694 | 0.713 | 0.730 | 0.741 | 0.747 | 0.750 | 0.751 | 0.751 |
| vs Radon 3 hr offset | 0.716 | 0.734 | 0.743 | 0.747 | 0.747 | 0.746 | 0.745 | 0.743 |

Figure (13): Environmental variable correlation with radon activity, Kemling Cave, Experiment 44, November 2013, evaluating changes in environmental variable integration time and radon offset to earlier times.

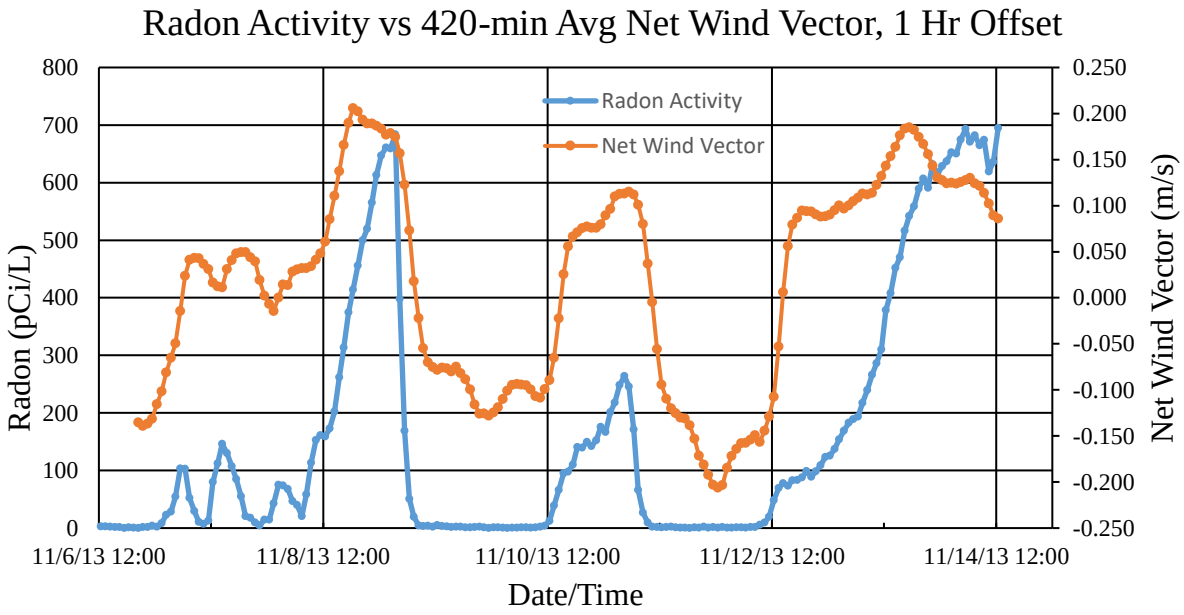


Figure (14): Overlay plot of radon activity offset 1 hour earlier vs. a 420-min average of net wind vector, Kemling Cave, Experiment 44, November 2013.

Returning to the issue of day/night subset correlations, these values were calculated from Experiments 35 and 44 and compared to those seen before from Experiment 20 in Figure (15). Conclusions that might have been drawn from the Experiment 20 subsets were largely confounded with the inclusion of repeat experiments at different times of the year. Whereas Experiment 20 (September) showed both pressure values correlating much more strongly during the daytime, Experiment 44 (November) shows the opposite and Experiment 35 (July) does not display greatly different subset behaviors. Surface density, surface temperature, and Δpressure did not significantly correlate with radon activity in July, but were significant in September and November, and more significant during the nighttime subset. The high-quality wind dataset from Experiment 44 produced significant correlations for all wind variables, yet did not show much variation in correlation between day and night.

## Conclusions

Surface temperature correlated positively with radon activity, but the correlation was only strong when the daily surface temperature straddled the cave temperature. July correlations were insignificant, and the strongest correlation was during September evenings, when cooling surface temperatures led to low radon activity in the cave entry passage. Surface density and Δpressure behaved in the same manner: not significantly correlated to radon activity in July, but significantly correlated in a negative manner during September and November, with the highest values also seen at night. Surface pressure and cave pressure formed strong and significant negative correlations with radon activity at all times of the year, with surface pressure

consistently yielding higher R values. The radon activity responded quickly to pressure changes with minimal delay time. Differences were seen when dividing the pressure response into day/night subsets, yet no simple trend could be discerned. The net wind vector, which factored in both the wind direction and velocity, produced the strongest and most important correlation with radon activity, but the radon activity response was delayed a few hours in contrast to the rapid responses seen to pressure changes. Longer integration periods did not improve the correlations of the environmental variables except for the wind parameters. However, for the high-quality wind data from Experiment 44, the improvement was only modest. It is important to note that these conclusions are probably only valid for a cave with open air communication with the environment, and where measurements were taken near the cave entrance and in the center of the passage cross-section. Further experiments probing the same cave using data from sites deeper in the cave and locations closer to the passage walls are in progress.

| **Exp 20, September** | **surf press** | **cave press** | **Δpress (surf - cave)** | **surf temp** | **surf wet air density** | **wind direct** | **wind velocity** | **net wind vector** |
|---|---|---|---|---|---|---|---|---|
| | | | | | | | | |
| **R overall** | -0.503 | -0.342 | -0.432 | 0.400 | -0.482 | | | |
| **R daytime** | -0.635 | -0.505 | -0.305 | 0.264 | -0.398 | | | |
| **R nighttime** | -0.291 | -0.147 | -0.599 | 0.664 | -0.671 | | | |

| **Exp 35, July** | **surf press** | **cave press** | **Δpress (surf - cave)** | **surf temp** | **surf wet air density** | **wind direct** | **wind velocity** | **net wind vector** |
|---|---|---|---|---|---|---|---|---|
| | | | | | | | | |
| **R overall** | -0.620 | -0.591 | 0.051 | 0.044 | -0.120 | -0.125 | 0.376 | 0.175 |
| **R daytime** | -0.659 | -0.638 | 0.069 | 0.138 | -0.219 | -0.148 | 0.500 | 0.254 |
| **R nighttime** | -0.581 | -0.530 | 0.045 | -0.188 | 0.041 | -0.114 | 0.229 | 0.032 |

| **Exp 44, November** | **surf press** | **cave press** | **Δpress (surf - cave)** | **surf temp** | **surf wet air density** | **wind direct** | **wind velocity** | **net wind vector** |
|---|---|---|---|---|---|---|---|---|
| | | | | | | | | |
| **R overall** | -0.476 | -0.446 | -0.281 | 0.168 | -0.272 | -0.548 | 0.240 | 0.623 |
| **R daytime** | -0.240 | -0.206 | -0.187 | 0.057 | -0.117 | -0.509 | 0.227 | 0.561 |
| **R nighttime** | -0.602 | -0.569 | -0.423 | 0.323 | -0.417 | -0.575 | 0.245 | 0.671 |

Figure (15): Environmental variable day/night subset correlations with radon activity at different times of the year, Kemling Cave.

## Acknowledgements

This study would not have been possible without the generous access privileges granted by the landowners of the study caves. Knox College provided financial support to enable this research. Experimental and theoretical assistance was provided by Chris Poe, Ed Klausner, Frank McAndrew, and Jerry Goodin. Special thanks to Eugene Welch for his role in designing and constructing the WindSonic interface hardware and to the folks at Rad Elec for their assistance.

## References

Eheman, C., Carson, B., Rifenburg, J., and Hoffman, D., 1991. Occupational Exposure to Radon Daughters in Mammoth Cave National Park. Health Physics, 60, 831-835.

Hakl, J., Csige, I., Hunyadi, I., Varhegyi, A., and Géczy, G., 1996. Radon Transport in Fractured Porous Media – Experimental Study in Caves. Environment International, 22, S433-S437.

Hakl, J., Hunyadi, I., Csige, I., Géczy, G., Lénárt, L., and Várhegyi, A., 1997. Radon Transport Phenomena Studied in Karst Caves – International Experiences on Radon Levels and Exposures. Radiation Measurements, 28, 675-684.

Jovanovič, P., 1996. Radon Measurements in Karst Caves in Slovenia. Environment International, 22, S429-S432.

Klausner, E., 2018. Personal Communication.

Kotrappa, P., Paul, P., Stieff, A., and Stieff, F., 2013. Measurement of Indoor and Outdoor Radon Concentrations During Superstorm Sandy. Radiation Protection Dosimetry, 157, 455-458.

Kowalczk, A.J., and Froelich, P.N., 2010. Cave Air Ventilation and $CO_2$ Outgassing by Radon-222 Modeling: How fast do caves breathe? Earth and Planetary Science Letters, 289, 209-219.

Langridge, D., Stokes, R.P., and Jackson, C.P., 2010. Monitoring of Radon Gas in Caves of the Yorkshire Dales, United Kingdom. Journal of Radiological Protection, 30, 545-556.

Lario, J., Sánchez-Moral, S., Cañaveras, J.C., Cuezva, S., and Soler, V., 2005. Radon Continuous Monitoring in Altamira Cave (Northern Spain) to Assess User's Annual Effective Dose. Journal of Environmental Radioactivity, 80, 161-174.

Lively, R.S., and Krafthefer, B.C., 1995. $^{222}Rn$ Variations in Mystery Cave, Minnesota. Health Physics, 68, 590-594.

Omnicalculator, 2018. Air Density Calculator. https://www.omnicalculator.com/physics/air-density. Accessed 5 July, 2018.

Palmer, A.N., 2007. Cave Geology. Cave Books, Dayton, OH.

Pinza-Molina, C., Alcaide, J.M., Rodriguez-Bethencourt, R., and Hernandez-Armas, J., 1999. Radon Exposures in the Caves of Tenerife (Canary Islands). Radiation Protection Dosimetry, 82, 219-224.

Rovenska, K., and Thinova, L., 2010. Seasonal Variation of Radon in the Bozkov Cave. Nukleonika, 55, 483-489.

Stieff, A., Kotrappa, P., and Stieff, F., 2012. The Use of Barrier Bags with Radon Detectors. Proceedings of the 2012 International Radon Symposium, pp. 67-79. http://aarst-nrpp.com/proceedings/2012/04_THE_USE_OF_BARRIER_BAGS_WITH_RADON_DETECTORS.pdf. Accessed 5 July, 2018.

Weather Underground, 2018. Weather history for the Dubuque Regional Airport. https://www.wunderground.com/history/airport/KDBQ. Accessed 30 June, 2018.

Welch, L.E., Paul, B.E., and Jones, M.D., 2015. Measurement of Radon Levels in Caves: Logistical Hurdles and Solutions. Proceedings of the 2015 International Radon Symposium, pp. 1-17. http://aarst-nrpp.com/proceedings/2015/MEASUREMENT_OF_RADON LEVELS_IN_CAVES LOGISTICAL_HURDLES_AND_SOLUTIONS.pdf. Accessed 5 July, 2018.

Welch, L.E., Paul, B.E., and Jones, M.D., 2016. Use of Electret Ionization Chambers to Measure Radon in Caves. Proceedings of the 2016 International Radon Symposium, pp. 1-18. http://aarst-nrpp.com/proceedings/2016/Welch_USE_OF_ELECTRET IONIZATION_CHAMBERS_TO_MEASURE_RADON_IN_CAVES.pdf. Accessed 5 July, 2018.

Welch, L.E., Paul, B.E., Miller, E.C., Chen, Y.I., Jones, M.D., and Beck, C.L., 2017. Depth Profiling of Radon in Vertical Shafts Using Electret Ionization Chambers. Proceedings of the 2017 International Radon Symposium, pp. 1-18. http://http://aarst-nrpp.com/proceedings/2017/DEPTH-PROFILING-OF-RADON-IN-VERTICAL-SHAFTS-USING-ELECTRET-IONIZATION-CHAMBERS-WELCH.pdf. Accessed 5 July, 2018.